Biochemical Pharmacology, Vol. 55, pp. 455–464, 1998.

ISSN 0006-2952/98/$19.00 + 0.00
PII S0006-2952(97)00483-8

Heterogeneous Forms of Adenotin-1 of Different Subcellular Localization

Anna Lorenzen, Jürgen Engelhardt, Birgit Kerst and Ulrich Schwabe

UNIVERSITÄT HEIDELBERG, PHARMAKOLOGISCHES INSTITUT, IM NEUENHEIMER FELD 366, D-69120 HEIDELBERG, GERMANY

ABSTRACT. The localization of the low-affinity adenosine binding protein adenotin-1 with respect to distribution in rat organs and subcellular compartments was investigated. Adenotin-1 was characterized by 5′-*N*-ethylcarboxamido[2,8-^{3}H]adenosine ([^{3}H]NECA) binding and Western blotting. Cytosolic as well as membrane fractions of all tissues contained adenotin-1. Highest levels of membrane-bound adenotin-1 were found in the liver (liver > kidney ≈ spleen ≈ lung > forebrain ≈ cerebellum > fat ≈ heart ≈ striated muscle), whereas highest levels of cytosolic adenotin-1 were detected in spleen, liver, lung and fat. Subcellular fractions from rat liver were prepared by differential and density gradient centrifugation. Like the homologous proteins endoplasmin or gp96, adenotin-1 is enriched in the endoplasmic reticulum. Cytosolic and membrane-bound adenotin-1 species are pharmacologically distinct, because in the liver particulate fraction adenotin-1 showed a more rapid binding kinetics, a twofold lower affinity for [^{3}H]NECA (K_D 227 nM vs. 105 nM) and a sevenfold higher affinity for 2-chloroadenosine than the cytosolic protein (K_i 1.48 μM vs. 9.25 μM). In rat liver cytosol, two different binding sites were found, which differed in [^{3}H]NECA binding kinetics and displayed a hundredfold difference in their affinity for 2-chloro-5′-*N*-methylcarboxamidoadenosine (K_i 45.8 nM vs. 4.76 μM). The presence of adenotin-1 in subcellular fractions, as determined by radioligand binding, was confirmed by Western blotting. Adenotin-1 was detected as a 98-kDa band in all rat liver subcellular fractions, which agrees with the molecular mass determined for the purified protein. In the cytosol, a 65-kDa band was labeled more intensely than the 98-kDa band. This additional band probably represents the pharmacologically distinct species of adenotin-1 found in the cytosol. BIOCHEM PHARMACOL 55;4:455–464, 1998. © 1998 Elsevier Science Inc.

KEY WORDS. adenotin; NECA; rat liver; radioligand binding; grp94 homologue; adenosine binding protein

Adenotin-1 is a ubiquitous protein which was initially characterized as an adenosine binding protein distinct from G-protein-coupled adenosine receptors [1–6]. The pharmacological profile of adenotin-1 differs from that of adenosine receptors, namely in its lack of affinity for adenosine receptor antagonists and N^6-substituted agonists [7]. Another adenosine-binding membrane protein is pharmacologically distinct from adenotin-1, because it also binds inosine and adenine nucleotides with high affinity [8]. In contrast, adenotin-2 is a recently described additional adenosine binding protein which is localized in cytosolic as well as in particulate subcellular compartments [9]. Adenotin-2 shares with adenotin-1 the lack of affinity for N^6-substituted agonists and xanthines. It can be distinguished from adenotin-1 pharmacologically because it is not sensitive to C1A†, but instead interacts with cyclic AMP in nanomolar concentrations. Adenotin-1 has a low affinity of approximately 20 μM for adenosine [10–12]. Purification from human placenta [10, 11] and human platelets [12] revealed a glycoprotein nature of this protein and a molecular mass of 98 kDa. The amino-terminal amino acid sequence of purified adenotin-1 is highly homologous to the N-terminus of the endoplasmic reticulum protein grp94 [11, 12]. As pointed out by Munro and Pelham [13], grp94 from different species has also been referred to as endoplasmin [14], ERp99 [15, 16], and hsp108 [17]. Grp94 is probably also identical to gp96 [18] and CaBP4 [19]. Furthermore, a considerable homology of adenotin-1 with a 98-kDa protein kinase from porcine brain microvessels was observed [20, 21].

Interestingly, unlike the closely related heat shock protein family, glucose-regulated proteins such as grp94 are not induced by high temperatures, but rather by oxygen deprivation, low extracellular pH and the presence of malfolded proteins in the ER [22, 23]. In hypoxic states such as ischemia, which lead to induction of grp94, tissue concentrations of adenosine are elevated [24]. These concentrations are probably also sufficient for occupation of adenosine binding sites of adenotin-1. In a fashion parallel to grp94 in neural cells, which is induced by ethanol [25],

* Corresponding author: Dr. A. Lorenzen, Institute of Pharmacology, University of Heidelberg, Im Neuenheimer Feld 366, 69120 Heidelberg, Germany. TEL. +49 6221 548 561; FAX +49 6221 548 644; E-mail anna.lorenzen@urz.uni-heidelberg.de

†*Abbreviations*: CHAPS, 3-[3-(cholamidopropyl)-dimethylammonio]-1-propanesulfonate; C1A, 2-chloro-adenosine; C1MECA, 2-chloro-5′-methylcarboxamidoadenosine; ER, endoplasmic reticulum; NECA, 5′-*N*-ethylcarboxamidoadenosine; R-PIA, R-N^6-phenylisopropyladenosine.

Received 28 March 1997; accepted 5 August 1997.

adenotin content of PC 12 cells is increased by ethanol exposure of the cells [26].

Diverse functional activities have been ascribed to grp94: a molecular chaperone activity [27–30], a role in antigen presentation and immunity against specific tumors, which requires ATPase activity [18, 31], an autophosphorylating activity [32], and the ability to bind calcium ions [19, 30]. The subcellular localization of grp94 is still controversial.

In the light of the close similarities of grp94 and adenotin-1 with respect to amino terminal sequences and conditions for induction, which may point to similar functions or even identity of these proteins, we studied the organ distribution and the subcellular localization of adenotin-1, also with respect to hypothetical isoforms in different cellular compartments, and compared it with the localization of grp94 (= endoplasmin, ERp99, hsp108, gp96, CaBP4). In addition to the membrane-associated form, soluble adenotin-1 was characterized previously in the cytosol of human placenta [11] and shown to consist of two isoforms with a molecular mass of 98 kDa and 74 kDa, respectively, but no pharmacological differences between these two forms were observed. In the present study, we have investigated if adenotin-1 is enriched in any subcellular particulate fraction or in cytosol. Adenotin-1 from different subcellular fractions was detected and characterized by radioligand binding and immunoblotting.

MATERIALS AND METHODS

Materials

[^{3}H]NECA (20–30 Ci/mmol) and UDP-[4,5-^{3}H]galactose (50 Ci/mmol) were obtained from NEN-Du Pont. Adenosine deaminase (from calf intestine; E.C. 3.5.4.4; 200 U/mg) and R-PIA were supplied by Boehringer. Monoclonal rat anti-chicken-grp94 (IgG_{2a}) antibody came from Biomol. Polyethyleneimine, C1A, CHAPS, and rabbit anti-rat IgG (peroxidase-coupled) were obtained from Sigma. Prepacked PD-10 gel filtration columns were purchased from Pharmacia. ECL™ Western blotting reagents, Hyperfilm™ ECL, and Rainbow™ molecular weight markers (14.3–220 kDa) were from Amersham-Buchler. GF/B glass fiber filters were purchased from Whatman. Nitrocellulose membranes (0.45 μm) came from Schleicher and Schuell. Purified adenotin-1 from human platelets was kindly provided by Dr. Thomas Fein, Institute of Pharmacology, University of Heidelberg, Germany. C1MECA was a generous gift from Prof. R. A. Olsson, Dept. of Internal Medicine, University of South Florida, Tampa, Florida. All other chemicals were from standard sources and of the highest purity commercially available.

Preparation of Soluble and Particulate Fractions from Rat Tissues

Male Sprague–Dawley rats (8–12 weeks old) were anaesthesized with ether and decapitated. Organs were quickly removed and stored on ice. All subsequent steps were performed at 0–4°. Organs were homogenized in 9 volumes of 0.32 M sucrose with a Polytron (Kinematika) for 20 sec (setting 6). The homogenate was centrifuged for 60 min at 100,000 × *g* in a Beckman Ti 60 rotor. The supernatant was used as cytosol and was aspirated, frozen in liquid nitrogen and stored at −75° until use. The pellet was washed twice after resuspension in 50 mM Tris-HCl, pH 7.4 and centrifugation for 60 min at 100,000 × *g* as described above. This crude membrane fraction was frozen in liquid nitrogen and stored at −75°.

Solubilization of Adenotin-1 from Crude Rat Liver Membranes

Membranes (10 mg/mL) were incubated with 0.4% (w/v) CHAPS in 50 mM Tris-HCl, pH 7.4, for 30 min on ice. After centrifugation for 30 min at 100,000 × *g* at 4°, the CHAPS concentration of the supernatant was reduced to 0.02% by gel filtration over prepacked PD-10 columns.

Preparation of Subcellular Organelles from Rat Liver

Rat liver homogenate was prepared and stored as described by Fleischer and Kervina [33]. Plasma membranes, nuclei, mitochondria, smooth and rough ER, and cytosol were enriched according to a published method [34]. Golgi fractions were isolated following the protocol of Tabas and Kornfeld [35]. Fractions were frozen in liquid nitrogen and stored at −75°.

Marker Enzymes and DNA Content

Enrichment of subcellular fractions was assessed by measurement of specific marker enzymes and DNA content. 5′-Nucleotidase (E.C. 3.1.3.5) [36, 37] was used as a marker for plasma membranes, lactate dehydrogenase (E.C. 1.1.1.27) for cytosol [38], fumarase (E.C. 4.2.1.2) for mitochondria [39], glucose-6-phosphatase (E.C. 3.1.3.9) for microsomes [40], UDP-galactosyltransferase (E.C. 2.4.1.38) for Golgi fractions [41], and DNA content for nuclei [42].

Protein Determination

Protein content of the samples was measured according to Peterson [43], using bovine serum albumin as reference protein.

Immunoblot Analysis of Adenotin-1 in Subcellular Fractions

Aliquots of the fractions (75 μg/lane) and purified adenotin-1 from human platelets (50 ng/lane) were subjected to SDS/PAGE [44], using Rainbow™ molecular weight markers (14.3–220 kDa), and transferred to nitrocellulose membranes in a semi-dry blotting device (TE 70 Semiphor™, Hoefer Scientific Instruments). Rat monoclonal anti-chicken-GRP-94 (IgG_{2a}, 2 μg/mL) was used as primary

antibody, which also detects purified adenotin-1.* Antigen-antibody complexes were visualized with peroxidase-coupled rabbit anti-rat-IgG (1:4000) using ECL™ Western blotting reagents and exposure of the membranes to Hyperfilm™ ECL.

Radioligand Binding

Radioligand binding was measured in a total volume of 250 μL in 50 mM Tris-HCl, pH 7.4 containing 0.02% (w/v) CHAPS, 0.2 U/mL adenosine deaminase, 10–200 μg sample protein, and 20 nM [^{3}H]NECA, if not indicated otherwise. Total binding to adenotin-1 was determined in the presence of 100 μM R-PIA, which suppresses binding of the radioligand to adenosine receptors. Nonspecific binding was determined by the addition of 100 μM CIA. All samples were incubated for 22 hr on ice, if not indicated otherwise. Incubations were terminated by filtration of 200 μL aliquots over glass fiber filters (GF/B), followed by washing with two 4 mL-portions of 50 mM Tris-HCl, pH 7.4. For the filtration of cytosolic and solubilized samples, filters had been impregnated with 0.3% (w/v) polyethyleneimine. Filters were transferred into scintillation vials, and 4 mL of scintillation cocktail (Aquasafe 300 Plus, Zinsser) was added. Radioactivity in the samples was determined in a Beckman LS 1801 liquid scintillation counter after equilibration of the samples for at least 6 hr at room temperature. All experiments were performed at least three times with duplicate samples.

Data Analysis

Equilibrium binding data from saturation and competition experiments were analyzed by nonlinear curvefitting using the SCTFIT Program [45]. Geometric means with 95% confidence limits are indicated for ligand affinities, and maximum binding capacities are given as arithmetic means ± SEM. Data from kinetic experiments were fitted as described previously [46] with the SigmaPlot program. Data were fitted to a two-site model, if fitting to two sites improved the fit significantly ($P < 0.05$) compared to a one-site model.

RESULTS

Localization of Adenotin-1

The adenotin-1 content of soluble and particulate fractions from seven different rat organs was determined by [^{3}H]NECA binding to adenotin-1 (Fig. 1). Adenotin-1 showed different distributions between soluble fractions and the crude membrane fractions. In crude membrane fractions from liver, radioligand binding to adenotin-1 (1921 ± 36 fmol/mg protein) exceeded the levels in other organs at least threefold. Lowest concentrations were measured in heart and muscle. In contrast, approximately equal

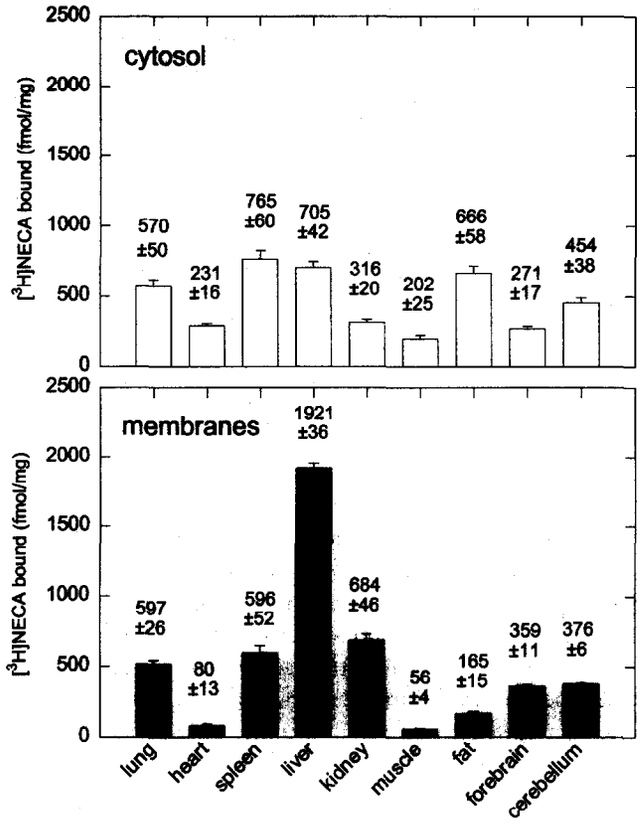

FIG. 1. Localization of adenotin-1 in rat tissues. The concentration of adenotin-1 in soluble (cytosol, upper panel) and particulate (crude membranes, lower panel) fractions from rat tissues (100 μg/tube) was determined by measurement of binding of 20 nM [^{3}H]NECA for 22 hr on ice. Total binding was measured in the presence of 100 μM R-PIA to inhibit radioligand binding to adenosine receptors, and nonspecific binding was determined in the presence of 100 μM CIA. Data are given as arithmetic means from three experiments ± SEM.

amounts of [^{3}H]NECA binding to adenotin-1 were measured in soluble fractions from lung (570 ± 50 fmol/mg), spleen (765 ± 60 fmol/mg), liver (705 ± 42 fmol/mg), fat (666 ± 58 fmol/mg), and cerebellum (454 ± 38 fmol/mg). Since highest concentrations of adenotin-1 were found in the liver, further characterization of this protein was performed in fractions from this organ.

Subcellular fractions from rat liver were prepared by differential and density gradient centrifugation. Specific marker enzyme activities indicated enrichment in the appropriate fractions (Table 1). Highest levels of radioligand binding to adenotin-1 were found in the smooth and rough endoplasmic reticulum, followed by plasma membranes, cytosol, mitochondria, Golgi fractions and nuclei (Fig. 2).

Pharmacological Characterization of Adenotin-1 Fractions

Since the enrichment of [^{3}H]NECA binding in ER might have been due to either an enrichment of the protein or to a higher affinity of adenotin-1 in this fraction compared to

* Fein et al., manuscript in preparation.

TABLE 1. Characterization of subcellular fractions from rat liver prepared by differential and density gradient centrifugation

	5'-NT mU/mg	LDH mU/mg	Fum mU/mg	DNA μg/mg	UDP-GT pmol/mg/min	Glc-6-P μmol P_i/mg/min
Homogenate	27.6 ± 6.3	1308 ± 78.8	448 ± 42.4	73.7 ± 13.4	4.1 ± 0.3	50.6 ± 2.5
Cytosol	12.0 ± 0.9	2466 ± 271	584 ± 32.1	23.6 ± 5.9	0.8 ± 0.1	6.7 ± 2.5
Nuclei	9.6 ± 4.8	49.6 ± 16.2	0.3 ± 0.2	1254 ± 194	0.8 ± 0.1	19.4 ± 0.7
PM	267 ± 31.3	84.7 ± 0.2	82.8 ± 30.1	61.2 ± 36.1	5.7 ± 3.7	32.2 ± 14.6
Mito R1	13.2 ± 8.0	48.9 ± 3.7	567 ± 61.7	73.4 ± 42.7	0.4 ± 0.1	6.9 ± 1.3
Mito R2	16.4 ± 3.2	151 ± 20.9	702 ± 121	30.6 ± 6.7	2.9 ± 2.2	21.7 ± 12.8
Smooth ER	99.9 ± 5.1	448 ± 93.4	58.2 ± 18.4	40.4 ± 7.8	7.6 ± 0.4	103 ± 6.9
Rough ER	17.7 ± 4.1	97.0 ± 34.5	43.7 ± 4.0	41.2 ± 8.8	1.9 ± 0.3	123 ± 6.6
Golgi	110 ± 35.1	98.7 ± 19.7	20.8 ± 8.0	15.0 ± 7.7	186 ± 28.0	40.5 ± 6.5

Marker enzymes and DNA content were measured in homogenate, cytosol, nuclei, plasma membranes (PM), mitochondria (mito), smooth and rough ER, and Golgi fractions. Results are given as means ± SEM from three preparations. 5'-NT, 5'-nucleotidase; LDH, lactate dehydrogenase; Fum, fumarase; UDP-GT, UDP-galactosyltransferase; Glc-6-P, glucose-6-phosphatase.

other subcellular compartments, we performed [^{3}H]NECA saturation experiments and determined the affinity for the radioligand and the maximum binding capacity in the homogenate, cytosol, and smooth and rough ER (Fig. 3). Scatchard plots indicated that adenotin-1 in the homogenate and the two ER fractions showed a uniform affinity for the ligand, whereas adenotin-1 in the cytosol had a twofold higher affinity (225, 205, and 241 nM in homogenate, smooth and rough ER respectively, and 105 nM in cytosol; $P < 0.005$ vs. homogenate, $P < 0.05$ vs. smooth and rough ER). Therefore, when measured at single radioligand concentrations, the levels of adenotin-1 are overestimated in the cytosol. Since the affinities of adenotin-1 for [^{3}H]NECA were not different between homogenate and the ER fractions, binding levels indicate a significant enrichment in the ER, which is supported by the higher B_{max} values in ER determined in saturation experiments.

Because the saturation experiments indicated that adenotin-1 in cytosol and in particulate fractions might be pharmacologically different, we investigated the radioligand binding characteristics more closely in kinetic studies and in competition experiments. Kinetics of [^{3}H]NECA binding were markedly different between cytosolic and crude membrane fractions (Fig. 4). Whereas binding to membranes reached equilibrium after one hour incubation and followed a monophasic association and dissociation, binding to the cytosolic adenotin-1 was much slower. In addition, the data both for the association and the dissociation were better fitted with a two-site than a one-site model, indicating the presence of two kinetically different [^{3}H]NECA binding sites on adenotin-1, or two different adenotin-1 subtypes in the cytosol. In order to investigate if these different kinetic properties were merely due to the different location of adenotin-1 in the cytosol, crude

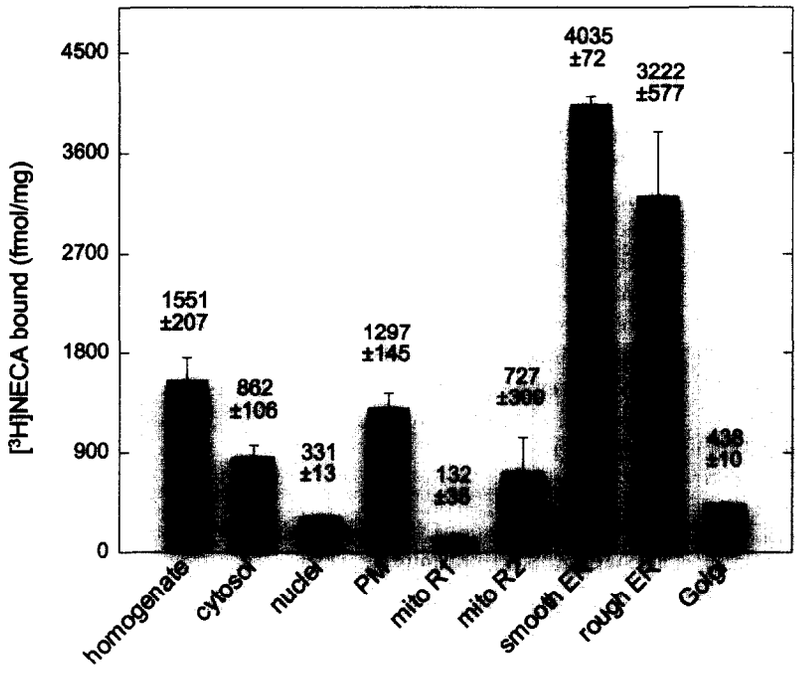

FIG. 2. Subcellular localization of adenotin-1. Subcellular fractions (cytosol, nuclei, mitochondria fractions R1 and R2, smooth and rough ER, Golgi) were prepared from rat liver homogenate as described in the experimental section. The enrichment of adenotin-1 in specific fractions was measured by determination of [^{3}H]NECA binding (20 nM) to the fractions (10–200 μg protein/tube). The data are from three preparations and are given as arithmetic means ± SEM.

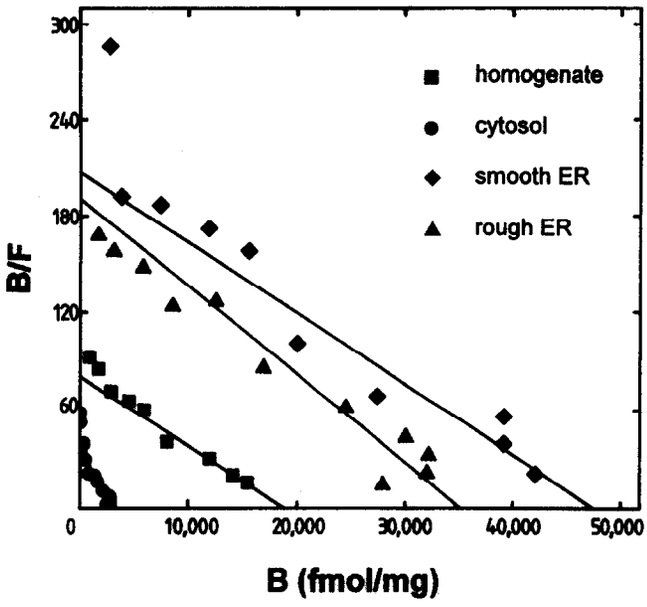

FIG. 3. Saturation of adenotin-1 with [^{3}H]NECA. 20–150 μg of homogenate (■), smooth (◆) or rough ER (▲), or cytoplasmic fractions (●) were incubated with 1–1000 nM [^{3}H]NECA. K_D and B_{max} values were determined by nonlinear curvefitting and indicated the presence of a single binding site in each preparation. The following parameters were obtained: homogenate: K_D 225 (213–238) nM, B_{max} 17,250 ± 1,110 fmol/mg; cytosol: K_D 105 (84–132) nM, B_{max} 3,480 ± 200 fmol/mg; smooth ER: K_D 205 (152–277) nM, B_{max} 48,020 ± 1,750 fmol/mg; rough ER: 241 (173–334) nM, B_{max} 37,610 ± 2,010 fmol/mg. K_D values are given as geometric means with 95% confidence limits, and B_{max} values as arithmetic means ± SEM from three different preparations.

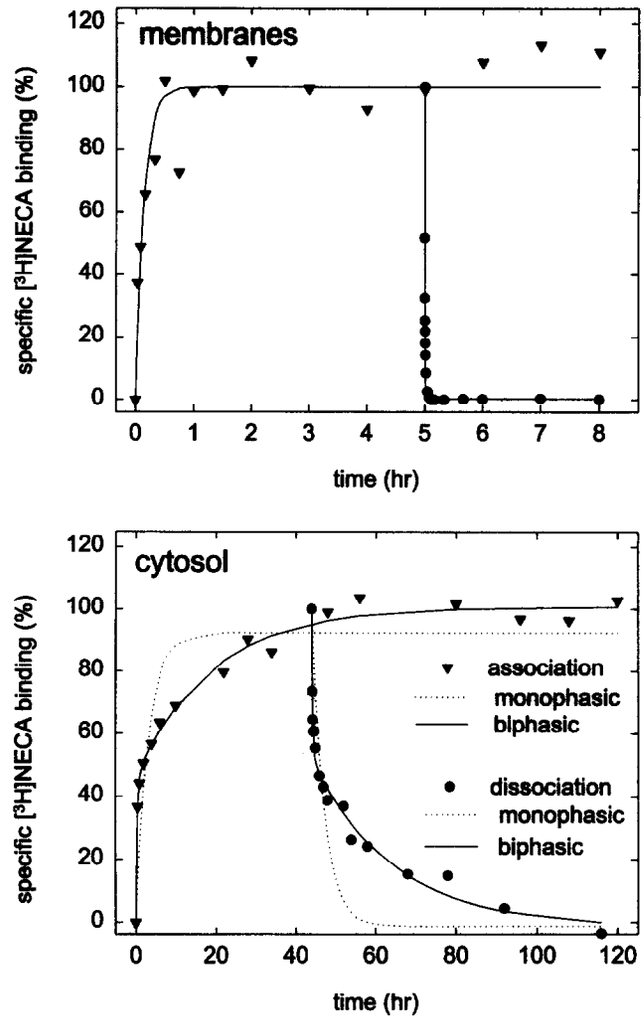

FIG. 4. Kinetics of [^{3}H]NECA binding to adenotin-1. [^{3}H]NECA binding (20 nM) to 100 μg membrane protein (upper) or 150 μg cytosolic protein (lower) on ice was determined after different incubation times. Dissociation of the radioligand was induced by the addition of 100 μM C1A. Nonlinear curvefitting yielded a monophasic curve for membranes (k_{-1} 0.134 ± 0.009 min^{-1}, k_{obs} 2.92 ± 0.163 min^{-1}) and biphasic association and dissociation curves for the cytosol (k_{-1A} 0.140 ± 0.043 min^{-1}, k_{-1B} 0.001 ± 0.0001 min^{-1}; k_{obsA} 0.046 ± 0.001 min^{-1}, k_{obsB} 0.001 ± 0.0001 min^{-1}).

membranes were solubilized with the zwitterionic detergent CHAPS. Since previous investigations [12] had shown that optimal solubilization of adenotin-1 was accomplished by CHAPS concentrations below the critical micellar concentration of the detergent, we used 0.4% CHAPS in the present study. The time-course of radioligand binding to adenotin-1 was compared in the cytosol, crude membranes, and the solubilized preparation. As shown in Fig. 5, membrane-bound and solubilized adenotin-1 showed identical time-courses of [^{3}H]NECA binding, which indicates that the different kinetic properties are not simply due to the different locations of adenotin-1 with respect to association to membranes. Protease inhibitors (1 μM leupeptin, 1 μM pepstatin, 100 μM phenymethylsulfonyl fluoride, 100 μM EDTA, 10 μg/mL amastatin and 10 μg/mL bestatin) did not affect the different [^{3}H]NECA binding characteristics in the cytosolic, crude membrane or solubilized preparation, indicating that the pharmacological differences were not due to proteolysis of adenotin during the preparation or binding assay.

Soluble and membrane-associated adenotin-1 were characterized in more detail in inhibition studies of radioligand binding with [^{3}H]NECA (Fig. 6). Membrane-associated adenotin-1 in crude membranes and membranes of the smooth ER displayed identical pharmacological profiles (Table 2). Monophasic inhibition curves were obtained for C1MECA (K_i 27.9 nM in crude membranes, 24.9 nM in smooth ER), NECA (K_i 296 nM in crude membranes, 264 nM in smooth ER) and C1A (K_i 1.48 μM in crude membranes, 1.29 μM in smooth ER). The pharmacological characteristics of adenotin-1 in the cytosol were significantly different from that of the membrane-associated protein (Table 2). NECA (K_i 113 nM) was twofold more potent in the cytosol than in membranes ($P < 0.0005$), whereas the potency of C1A (K_i 9.25 μM) was significantly lower in the cytosol ($P < 0.0001$). The inhibition of [^{3}H]NECA binding in the cytosol by C1MECA revealed

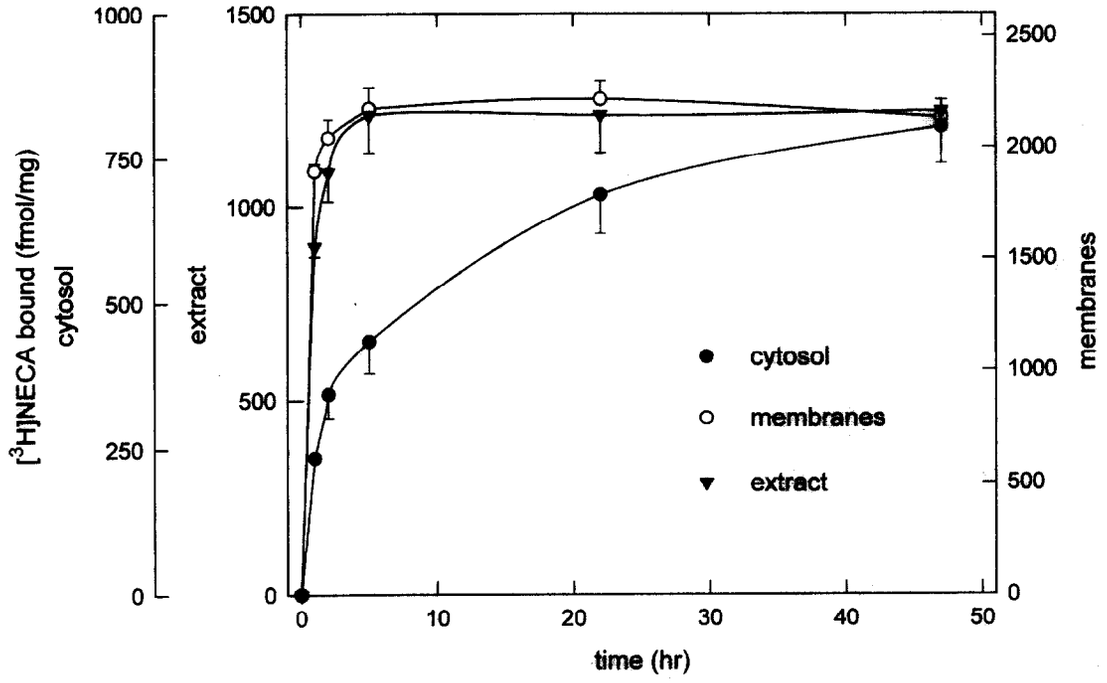

FIG. 5. Time-course of [^{3}H]NECA binding to adenotin-1 in particulate and soluble preparations and in a solubilized extract. Adenotin-1 was solubilized from crude membranes from rat liver with 0.4% CHAPS as described in the experimental section. Radioligand binding (20 nM [^{3}H]NECA) to adenotin-1 was compared in crude membranes, cytosol, and in the solubilized preparation. Incubations were performed on ice for up to 48 hr.

the presence of two different binding sites. Thirty-six percent of radioligand binding was inhibited by ClMECA with a K_i value of 45.8 nM, which is twice as high as the K_i value measured in membranes. The residual [^{3}H]NECA binding was inhibited by this compound with a K_i value of 4.76 μM.

Immunoblotting of Adenotin-1

The notion that adenotin-1 in the cytosol and in a membrane-associated state are not identical, which was suggested by pharmacological differences, was further corroborated by immunological characterization of adenotin-1 of different subcellular localization. Western blotting revealed adenotin-1 bands of different molecular mass in various subcellular compartments (Fig. 7). Two major bands of 98 and 65 kDa were detected in all fractions. In homogenate and plasma membranes, both forms were present, yielding bands of approximately identical densities. In smooth and rough ER, the 98 kDa form was clearly predominant, whereas in the cytosol the 65 kDa band comprised the major form. Nuclei contained five major and two minor bands. In addition to the 98- and the 65-kDa band, five further bands were observed in this fraction (Fig. 7). The identity of these additional bands cannot be stated presently.

Taken together, these results indicate that adenotin-1 occurs in different isoforms, which differ in their subcellular localization, their pharmacological properties and in molecular mass.

DISCUSSION

The presence of adenotin-1 has been demonstrated in a variety of different tissues, e.g. human placenta [1], human platelets [2, 7], mouse mastocytoma cells [3], pig smooth muscle cells [4] and rat cerebral cortex [5]. However, the relative abundance of adenotin-1 in tissues is difficult to assess due to the different species investigated. In the present study, we have investigated the localization of adenotin-1 with respect to possible enrichment in rat tissues and subcellular compartments, because this may point to the physiologically relevant site of action of this protein. Since the amino-terminal amino acid sequence of adenotin-1 is highly homologous to grp94 and related or identical proteins [11, 12] such as endoplasmin, gp96, ERp99 or hsp108, it seemed interesting to compare the localization of adenotin-1 to the localization of these proteins. We have further performed pharmacological characterization of adenotin-1 with respect to possible heterogeneity.

When measured by [^{3}H]NECA binding, highest concentrations of adenotin-1 were detected in membranes of tissues rich in endoplasmic reticulum (Fig. 1), a similar distribution as found previously for the homologous protein endoplasmin [14]. In membranes, levels of [^{3}H]NECA binding to adenotin-1 were, in decreasing order: liver $\gg$ kidney $\approx$ spleen $\approx$ lung $>$ forebrain $\approx$ cerebellum $>$ fat $\approx$ heart $\approx$ striated muscle. Whole cell extracts contained highest concentrations of endoplasmin in liver and pancreas, intermediate levels in lung, spleen, kidney, heart and muscle, and lowest amounts in brain [14], as assessed by

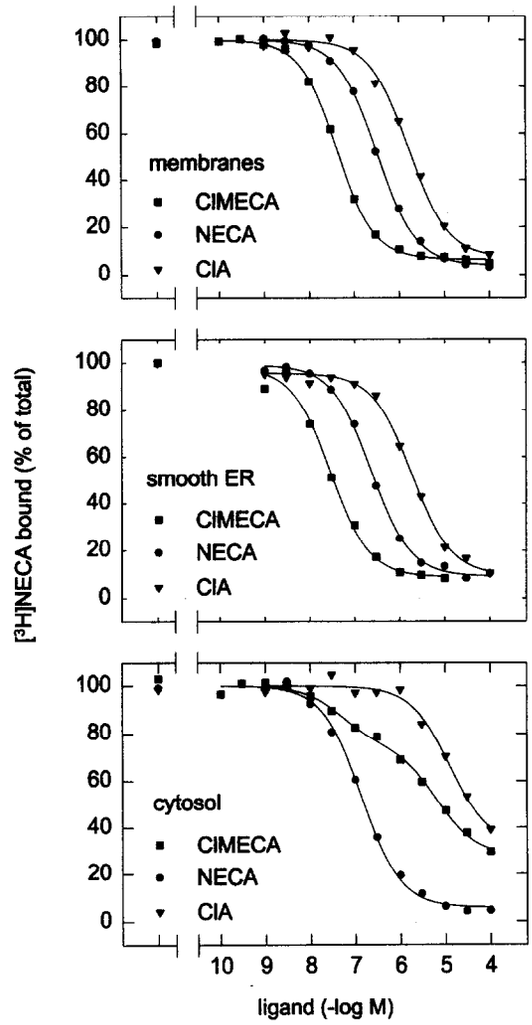

FIG. 6. Competition for [^{3}H]NECA binding to adenotin-1 by adenosine derivatives. Radioligand binding (20 nM [^{3}H]NECA; incubation for 24 hr on ice) to crude membranes (upper panel), smooth ER fractions (center) from density gradient centrifugation, and cytosol (lower) was displaced by increasing concentrations of NECA, C1A, and C1MECA. Nonlinear curve-fitting yielded monophasic inhibition curves for all compounds in all preparations except for C1MECA in the cytosol. The following K_i values were calculated: Membranes: NECA 296 nM (95% confidence limits: 261–337 nM), C1A 1.48 (1.40–1.56) μM, C1MECA 27.9 (25.1–31.1) nM; smooth ER: NECA 264 (197–353) nM, C1A 1.29 (0.97–1.71) μM, C1MECA 24.9 (22.7–27.4) nM; cytosol: NECA 113 (108–118) nM, C1A 9.25 (7.77–11.2) μM, C1MECA 45.8 (32.2–65.3) nM (high affinity; 36% of the binding sites in cytosol) and 4.76 (3.39–6.70) μM (low affinity).

immunoblotting with antibodies to endoplasmin. Chicken hsp108 showed an identical localization [47]. Considerable concentrations of adenotin-1 were also found in cytosolic fractions (Fig. 1). Unlike in membranes, the adenotin-1 content in cytosolic fractions from liver did not greatly surpass the content in cytosol from other tissues.

The subcellular localization of adenotin-1 was investigated in fractions from rat liver after differential and density gradient centrifugation. The subcellular distribution of adenotin-1 (Fig. 2) resembles the distribution of endoplasmin [14], ERp99 [15], CaBP4 [19] and grp94 [48], because highest concentrations of all proteins are found in ER. These homologous proteins contain a carboxyterminal KDEL sequence, which acts as a retention signal for the ER [13]. In spite of this retention signal, endoplasmin and homologues have also been found in the plasma membrane [49] and in the Golgi apparatus before secretion into the extracellular space [50]. The tumor rejection antigen gp96 was also found in cytosolic and particulate fractions [51]. In a similar way, lower concentrations of adenotin-1 have also been detected in non-ER subcellular fractions (Fig. 2). Plasma membranes and cytosol contained approximately three- and fivefold lower levels of adenotin-1 than smooth ER.

Saturation experiments performed with [^{3}H]NECA confirmed that the higher quantity of binding to ER fractions compared to the homogenate (Fig. 2) was due to an authentic enrichment of adenotin-1 in these fractions. K_D values in smooth and rough ER fractions were identical to the K_D value of adenotin-1 in the homogenate, and B_{max} values revealed an approximately threefold enrichment of this protein in ER. [^{3}H]NECA saturation in the cytosol disclosed a significantly higher affinity of cytosolic adenotin-1 for the radioligand than the membrane-bound form (Fig. 3 and Table 2). We took this as an indication that cytosolic and membrane-associated adenotin-1 may not be identical. Therefore, we further studied possible heterogeneities between cytosolic and membrane-associated forms of adenotin-1 in kinetic experiments with [^{3}H]NECA (Fig. 4). In crude membranes, [^{3}H]NECA association and dissociation were very rapid and followed a monophasic time-course, which is in agreement with the kinetics observed for adenotin-1 solubilized from human platelet membranes [7]. In contrast, [^{3}H]NECA binding to cytosolic adenotin-1 was a biphasic process and much slower than in membranes. This finding is not consistent with the results of saturation experiments, which revealed the presence of a single binding site only. However, differences in affinity may be too small to be detected by saturation studies. Alternatively, the two sites found in kinetic studies may even have identical K_D values, because the K_D is calculated as the ratio of k_{-1} and k_{+1}. The observed differences in kinetics were not due to membrane association or cytosolic localization, respectively, because adenotin-1 showed identical kinetics in the membrane-associated state as well as after solubilization (Fig. 5). We do not attribute the appearance of different forms of adenotin-1 to proteolysis during the experiment, because protease inhibitors (1 μM leupeptin, 1 μM pepstatin, 100 μM phenylmethylsulfonyl fluoride, 100 μM EDTA, 10 μg/mL amastatin and 10 μg/mL bestatin) were without effect. Proteolysis may have occurred within the intact cells.

We subsequently performed pharmacological characterization of adenotin-1 from different compartments, and the results are summarized and compared to the results of other investigators in Table 2. Evidence for the presence of two

TABLE 2. Comparison of pharmacological profiles of adenotin-1 from different sources

	Placenta[a]		Platelet[b]		Liver	
	Membranes	Cytosol	Membranes	Crude membranes	Smooth ER	Cytosol
[^{3}H]NECA	210	220	155	227 (176–294)	205 (152–277)	105* (84–132)
NECA	370	180	182	296 (261–337)	264 (197–353)	113** (108–118)
C1A	1,800	1,500	1,090	1,480 (1,400–1,560)	1,290 (974–1,712)	9,250*** (7,770–11,200)
C1MECA	n.d.[c]	n.d.[c]	18	27.9 (25.1–31.1)	24.9 (22.7–27.4)	45.8 (64%) (32.2–65.3) 4,760 (36%) (3,390–6,700)

Adenotin-1 was characterized by [^{3}H]NECA binding in crude membranes, smooth ER and cytosol from rat liver (present investigation) and after purification from membrane or cytosolic fractions of human placenta [11] and membranes of human platelets [12]. K_D and K_i values with 95% confidence limits are given in nmol/L. [a]Data from ref. [11]; [b]data from ref. [12]; [c]n.d., not determined. *$P < 0.01$ vs. liver crude membranes; **$P < 0.0005$ vs. liver crude membranes; ***$P < 0.0001$ vs. liver crude membranes.

pharmacologically different subtypes of adenotin-1 in cytosol came from competition experiments (Fig. 6). By inhibition of radioligand binding with C1MECA, two binding sites with affinities of 46 nM and 4.76 μM for this adenosine analogue were detected, whereas C1MECA bound to a single site in membranes with higher affinity than to the high-affinity site in cytosol.

Competition experiments also provided evidence that membrane-associated adenotin-1 is distinct from cytosolic adenotin-1. The difference in affinity for NECA observed in saturation experiments with the tritiated derivative was confirmed in the inhibition studies. In addition, it was shown that C1A, although it did not discriminate the two cytosolic forms of adenotin-1, displayed a significantly higher affinity for the membrane-associated than for the cytosolic protein (Table 2).

The pharmacological characteristics of membrane-associated adenotin-1 from rat liver described in the present study are identical to the characteristics of adenotin purified from human placental membranes [11]. However, there are relevant differences between the cytosolic forms of adenotin-1 from rat liver and the cytosolic forms of this protein from human placenta (Table 2). The affinities for [^{3}H]NECA of adenotin-1 purified from cytosolic and membrane fractions from human placenta were identical [11]. In contrast, adenotin-1 from rat liver showed a significantly higher affinity for the radioligand in the cytosol than the membrane-associated protein. A second difference between placental cytosolic adenotin-1 and rat liver cytosolic adenotin-1 was found in inhibition experiments with C1A. In rat liver cytosol, adenotin-1 showed an approximately sevenfold lower affinity for this adenosine analogue than the membrane-associated protein, whereas no such difference was found for placental adenotin-1. Heterogeneity of cytosolic adenotin-1 from rat liver was revealed in kinetic experiments with [^{3}H]NECA as well as in inhibition experiments with C1MECA. Kinetic studies and competition of C1MECA with [^{3}H]NECA binding have not been performed with cytosolic adenotin-1 from human placenta, and there is therefore no evidence for possible pharmacological differences between the two cytosolic forms from this tissue.

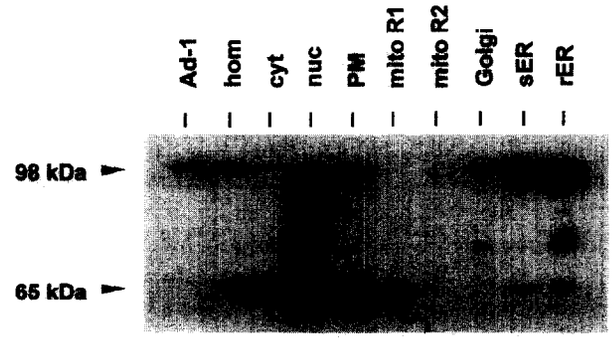

FIG. 7. Western blotting of adenotin-1 in subcellular fractions. Purified adenotin-1 (50 ng) and subcellular fractions (75 μg/lane) were subjected to 10% SDS-PAGE and transferred to nitrocellulose membranes. Adenotin-1 was detected by rat monoclonal anti-chicken-GRP-94 antibody (2 μg/mL) and visualized with peroxidase-coupled rabbit anti-rat-IgG (1:4000) using ECL™ Western blotting reagents. The molecular mass of the detected bands is indicated on the left. Ad-1, adenotin-1 purified from human platelets; hom, homogenate; cyt, cytosol; nuc, nuclei; PM, plasma membranes, mito, mitochondria; sER, smooth ER; rER, rough ER.

Adenotin-1 was further studied by immunoblotting of subcellular fractions using a monoclonal antibody against grp94 which binds to adenotin-1 purified from human platelet membranes, revealing a single band of 98-kDa molecular mass.* At 98 kDa, the antibody identified adenotin-1 in subcellular fractions, as estimated by [^{3}H]NECA binding (Fig. 7). The antibody also reacted with one major band of 65-kDa molecular mass, which was most prominent in cytosol (Fig. 7). Approximately equivalent amounts of the 65- and the 98-kDa proteins were found in the homogenate, whereas only one binding site was detected in this preparation by [^{3}H]NECA saturation (Fig. 3).

*Fein et al., manuscript in preparation.

As pointed out above, a twofold difference in affinity for the radioligand is probably too small to discriminate two binding sites in saturation studies. In addition, the affinity of the antibody for the 65- and 98-kDa forms may not be identical, and it is not known if equal staining densities actually reflect equal amounts of protein.

Proteolytic degradation of adenotin-1, which yielded a 74-kDa form, has been described in placental cytosol [11]. We assume, therefore, that the 65-kDa protein observed in the present study represents a fragment of adenotin-1. However, the sizes of the fragments from human placenta and rat liver are not identical. Therefore, it seems conceivable that the cytosolic forms from these two tissues may also differ pharmacologically, as shown in radioligand binding experiments. Molecular heterogeneity has also been described for the highly homologous protein gp96 [52]. Purified gp96 preparations from Meth A sarcoma cells, although containing identical C- and N-termini and exhibiting no differences in N-linked glycosylation, were found to be heterogeneous with respect to size, charge and reactivity with different antibodies. The differences in size of gp96 species (96-110 kDa) are much smaller than the size differences observed for adenotin-1 (65 and 98 kDa). Although it seems plausible that the 65-kDa band in rat liver cytosol (and also in much lower densities in other compartments) is identical with adenotin-1 from cytosol, which is also pharmacologically distinct, more direct evidence, e.g. amino acid sequencing, is necessary to determine the nature of this protein.

In conclusion, we have shown that adenotin-1 is highly enriched in rat liver ER membranes. In the cytosol, two different forms of adenotin-1 were identified. Membrane-associated and cytosolic species of adenotin-1 are distinct. These biochemically and pharmacologically distinct forms of adenotin-1 may have different physiological functions, which may be modulated by adenosine according to the respective susceptibility of the adenotin-1 isoform. Given the sequence homology to grp94, the similarity in organ distribution and the enrichment of both proteins in endoplasmic reticulum, one may speculate that the membrane-associated form of adenotin-1 possibly has a molecular chaperone function as well, which is enhanced under circumstances when adenosine concentrations are increased, e.g. hypoxia or ischemia. The role of the cytosolic forms of adenotin-1 is probably distinct. In analogy to grp94, to which numerous functions have been ascribed, such as molecular chaperone activity [27–30], antigen presentation and ATPase activity [18, 31], autophosphorylation [32] as well as the ability to bind calcium ions [19, 30], one may speculate that not all possible activities are equally and simultaneously exerted by a single protein under all physiological conditions in different cellular compartments. Rather, it seems reasonable to assume that a protein with several distinct functional activities may be microheterogenous, and that modifications of the molecule regulate the subcellular localization and the appropriate physiological activity. The physiological roles of adenotin-1 isoforms may likewise be influenced by subcellular localization and affinity for adenosine. For the understanding of the exact relationship between adenotin-1 and grp94 and its homologues, sequencing and cloning of adenotin-1 will be necessary.

The authors wish to thank Dr. Thomas Fein for the generous gift of purified adenotin-1 from human platelets.

References

1. Fox IH and Kurpis L, Binding characteristics of an adenosine receptor in human placenta. *J Biol Chem* **258:** 6952–6955, 1983.
2. Hüttemann E, Ukena D, Lenschow V and Schwabe U, R_a adenosine receptors in human platelets. Characterization by 5′-*N*-ethylcarboxamido[^{3}H]adenosine binding in relation to adenylate cyclase activity. *Naunyn-Schmiedebergs Arch Pharmacol* **325:** 226–233, 1984.
3. Nakata H and Fujisawa H, 5′-*N*-Ethylcarboxamide[^{3}H]-adenosine binding sites of mouse mastocytoma P815 cell membranes: characterization and solubilization. *J Biochem* **105:** 888–893, 1989.
4. Diocee DK and Souness JE, Characterization of 5′-ethylcarboxamido[^{3}H]adenosine binding to pig aorta smooth muscle membranes. *Biochem Pharmacol* **36:** 3621–3627, 1987.
5. Florio C, Traversa U, Vertua R and Puppini P, 5′-*N*-Ethylcarboxamido[8-^{3}H]adenosine binds to two different adenosine receptors in membranes from the cerebral cortex of the rat. *Neuropharmacology* **27:** 85–94, 1988.
6. Keen M, Kelly E, Nobbs P and McDermot JM, A selective binding site for ^{3}H-NECA that is not an adenosine A_2 receptor. *Biochem Pharmacol* **38:** 3827–3833, 1989.
7. Lohse MJ, Elger B, Lindenborn-Fotinos J, Klotz K-N and Schwabe U, Separation of solubilized A_2 adenosine receptors of human platelets from non-receptor [^{3}H]NECA binding sites by gel filtration. *Naunyn-Schmiedebergs Arch Pharmacol* **337:** 64–68, 1988.
8. Lorenzen A, Grün S, Vogt H and Schwabe U, Identification of a novel high affinity adenosine binding protein from bovine striatum. *Naunyn-Schmiedebergs Arch Pharmacol* **346:** 63–68, 1992.
9. Lorenzen A, Groæekatthöfer B, Kerst B, Vogt H, Fein T and Schwabe U, Characterization of a novel adenosine binding protein sensitive to cyclic AMP in rat brain cytosolic and particulate fractions. *Biochem Pharmacol* **52:** 1375–1385, 1996.
10. Hutchison KA and Fox IH, Purification and characterization of the adenosine A_2-like binding site from human placental membranes. *J Biol Chem* **264:** 19898–19903, 1989.
11. Hutchison KA, Nevins B, Perini F and Fox IH, Soluble and membrane-associated human low-affinity adenosine binding protein (adenotin): Properties and homology with mammalian and avian stress proteins. *Biochemistry* **29:** 5138–5144, 1990.
12. Fein T, Schulze E, Bär J and Schwabe U, Purification and characterization of an adenotin-like adenosine binding protein from human platelets. *Naunyn-Schmiedebergs Arch Pharmacol* **349:** 374–380, 1994.
13. Munro S and Pelham HRB, A C-terminal signal prevents secretion of luminal ER proteins. *Cell* **48:** 899–907, 1987.
14. Koch G, Smith M, Macer D, Webster P and Mortara R, Endoplasmic reticulum contains a common, abundant calcium-binding glycoprotein, endoplasmin. *J Cell Sci* **86:** 217–232, 1986.

15. Lewis MJ, Mazzarella RA and Green M, Structure and assembly of the endoplasmic reticulum. The synthesis of three major endoplasmic reticulum proteins during lipopoly-saccharide-induced differentiation of murine lymphocytes. *J Biol Chem* **260:** 3050–3057, 1985.
16. Mazzarella RA and Green M, ERp99, an abundant, conserved glycoprotein of the endoplasmic reticulum, is homologous to the 90-kDa heat shock protein (hsp90) and the 94-kDa glucose regulated protein (GRP94). *J Biol Chem* **262:** 8875–8883, 1987.
17. Kulomaa MS, Weigel NL, Kleinsek DA, Beattie WG, Conneely, OM, March C, Zarucki-Schulz T, Schrader WT and O'Malley BW, Amino acid sequence of a chicken heat shock protein derived from the complementary DNA nucleotide sequence. *Biochemistry* **25:** 6244–6251, 1986.
18. Maki RG, Old LJ and Srivastava PK, Human homologue of murine tumor rejection antigen gp96: 5′-Regulatory and coding regions and relationship to stress-induced proteins. *Proc Natl Acad Sci USA* **87:** 5658–5662, 1990.
19. Nguyen Van P, Peter F and Söling H-D, Four intracisternal calcium-binding glycoproteins from rat liver microsomes with high affinity for calcium. *J Biol Chem* **264:** 17494–17501, 1989.
20. Dechert U, Weber M, Weber-Schaeuffelen M and Wollny E, Isolation and partial characterization of an 80,000-Dalton protein kinase from the microvessels of the porcine brain. *J Neurochem* **53:** 1268–1275, 1989.
21. Dechert U, Weber P, König B, Ortwein C, Nilson I, Linxweiler W, Wollny E and Gassen HG, A protein kinase isolated from porcine brain microvessels is similar to a class of heat-shock proteins. *Eur J Biochem* **225:** 805–809, 1994.
22. Lee AS, Coordinated regulation of a set of genes by glucose and calcium ionophores in mammalian cells. *Trends Biochem Sci* **12:** 20–23, 1987.
23. Kozutsumi Y, Segal M, Normington K, Gething M-J and Sambrook J, The presence of malfolded proteins in the endoplasmic reticulum signals the induction of glucose-regulated proteins. *Nature* **332:** 462–464, 1988.
24. Hagberg H, Andersson P, Lacarewicz J, Jacobson I, Butcher S and Sandberg M, Extracellular adenosine, inosine, hypoxanthine, and xanthine in relation to tissue nucleotides and purines in rat striatum during transient ischemia. *J Neurochem* **49:** 227–231, 1987.
25. Miles MF, Wilke N, Elliot M, Tanner W and Shah S, Ethanol-responsive genes in neural cells include the 78-kilodalton glucose-regulated protein (grp78) and the 94-kilodalton glucose-regulated protein (grp94) molecular chaperones. *Mol Pharmacol* **46:** 873–879, 1994.
26. Rabin RA, Regulation of the stress-like protein adenotin in PC-12 cells by ethanol exposure. *Biochem Pharmacol* **51:** 183–186, 1996.
27. Navarro D, Qadri I and Pereira L, A mutation in the ectodomain of herpes simplex virus 1 glycoprotein B causes defective processing and retention in the endoplasmic reticulum. *Virology* **184:** 253–264, 1991.
28. Schaiff WT, Hruska KA Jr, McCourt DW, Green M and Schwartz BD, HLA-DR associates with specific stress proteins and is retained in the endoplasmic reticulum in invariant chain negative cells. *J Exp Med* **176:** 657–666, 1992.
29. Melnick J, Aviel S and Argon Y, The endoplasmic reticulum stress protein GRP94, in addition to BiP, associates with unassembled immunoglobulin chains. *J Biol Chem* **267:** 21303–21306, 1992.
30. Nigam SK, Goldberg AL, Ho S, Rohde MF, Bush KT and Sherman MY, A set of endoplasmic reticulum proteins possessing properties of molecular chaperones includes Ca^{2+}-binding proteins and members of the thioredoxin family. *J Biol Chem* **269:** 1744–1749, 1994.
31. Li Z and Srivastava PK, Tumor rejection antigen gp96/grp94 is an ATPase: implications for protein folding and antigen presentation. *EMBO J* **12:** 3143–3151, 1993.
32. Csermely P, Miyata Y, Schnaider T and Yahara I, Autophosphorylation of grp94 (endoplasmin). *J Biol Chem* **270:** 6381–6388, 1995.
33. Fleischer S and Kervina M, Long-term preservation of liver for subcellular fractionation. *Methods Enzymol* **31:** 3–6, 1974.
34. Fleischer S and Kervina M, Subcellular fractionation of rat liver. *Methods Enzymol* **31:** 6–41, 1974.
35. Tabas I and Kornfeld S, Purification and characterization of a rat liver Golgi alpha-mannosidase capable of processing asparagine-linked oligosaccharides. *J Biol Chem* **254:** 1655–11663, 1979.
36. Pletsch QA and Coffey JW, Studies on 5′-nucleotidases of rat liver. *Biochim Biophys Acta* **276:** 192–205, 1972.
37. Heinz F and Haeckel R, 5′-Nucleotidase, UV-method. In: *Methods of Enzymatic Analysis*, Vol. IV (Ed. Bergmeyer HU), pp. 113–120. Verlag Chemie, Weinheim, Deerfield Beach, Basel, 1984.
38. Vassault A, Lactate dehydrogenase, UV-method with pyruvate and NADH. In: *Methods of Enzymatic Analysis*, Vol. III (Ed. Bergmeyer HU), pp. 118–126. Verlag Chemie, Weinheim, Deerfield Beach, Basel, 1984.
39. Stitt M, Fumarase. In: *Methods of Enzymatic Analysis*, Vol. IV, (Ed. Bergmeyer HU), pp. 359–362. Verlag Chemie, Weinheim, Deerfield Beach, Basel, 1984.
40. Swanson MA, Glucose-6-phosphatase from liver. *Methods Enzymol* **3:** 541–543, 1955.
41. Verdon B and Berger EG, Galactosyltransferase. In: *Methods of Enzymatic Analysis*, Vol. III (Ed. Bergmeyer HU), pp. 374–381. Verlag Chemie, Weinheim, Deerfield Beach, Basel, 1984.
42. Labarca C and Paigen K, A simple, rapid, and sensitive DNA assay procedure. *Anal Biochem* **102:** 344–352, 1980.
43. Peterson GL, A simplification of the protein assay method of Lowry *et al.* which is more generally applicable. *Anal Biochem* **83:** 346–356, 1977.
44. Laemmli UK, Cleavage of structural proteins during the assembly of the head of bacteriophage T4. *Nature* **227:** 680–685, 1970.
45. De Lean A, Hancock AA and Lefkowitz RJ, Validation and statistical analysis of radioligand binding data for mixtures of pharmacological receptor subtypes. *Mol Pharmacol* **21:** 5–16, 1982.
46. Lohse MJ, Lenschow V and Schwabe U, Two affinity states of R_i adenosine receptors in brain membranes. *Mol Pharmacol* **26:** 1–9, 1984.
47. Sargan DR, Tsai M-J and O'Malley BW, Hsp108, a novel heat shock inducible protein of chicken. *Biochemistry* **25:** 6252–6258, 1986.
48. Cala SE and Jones LR, GRP94 resides within cardiac sarcoplasmic reticulum vesicles and is phosphorylated by casein kinase II. *J Biol Chem* **269:** 5926–5931, 1994.
49. Takemoto H, Yoshimori T, Yamamoto A, Miyata Y, Yahara I, Inoue K and Tashiro Y, Heavy chain binding protein (BiP/GRP78) and endoplasmin are exported from the endoplasmic reticulum in rat exocrine pancreatic cells, similar to protein disulfide-isomerase. *Arch Biochem Biophys* **296:** 129–136, 1992.
50. Booth C and Koch GLE, Perturbation of cellular calcium induces secretion of luminal ER proteins. *Cell* **59:** 729–737, 1989.
51. Srivastava PK, DeLeo AB and Old LJ, Tumor rejection antigens of chemically induced sarcomas of inbred mice. *Proc Natl Acad Sci USA* **83:** 3407–3411, 1986.
52. Feldweg AM and Srivastava PK, Molecular heterogeneity of tumor rejection antigen/heat shock protein gp96. *Int J Cancer* **63:** 310–314, 1995.